Self-assembling properties of non-ionic tetraphenylporphyrins and discotic phthalocyanines carrying oligo(ethylene oxide) alkyl or alkoxy units

Johannes M. Kroon,[a] Robert B. M. Koehorst,[b] Marinus van Dijk,[a] Georgine M. Sanders[a] and Ernst J. R. Sudhölter*[,a]

[a]*Department of Organic Chemistry, Wageningen Agricultural University, Dreijenplein 8, 6703 HB Wageningen, The Netherlands*

[b]*Department of Molecular Physics, Wageningen Agricultural University, Dreijenlaan 5, 6703 HA Wageningen, The Netherlands*

The thermotropic phase behaviour and self-assembling features of some non-ionic tetraphenylporphyrins and phthalocyanines containing oligo(ethylene oxide) alkoxy or alkyl units have been investigated. From DSC measurements and polarization microscopy it was concluded that none of the tetraphenylporphyrins was mesomorphic while the phthalocyanines displayed discotic hexagonal phases even at room temperature. The aggregation of the compounds in aqueous media was studied by means of UV–VIS and fluorescence spectroscopy and it has been found that in water the tetraphenylporphyrins form J- or head-to-tail type of aggregates while phthalocyanines form H- or face-to-face type of aggregates. The luminescence properties of the tetraphenylporphyrin and phthalocyanine aggregates are explained on the basis of the molecular exciton approximation. Steric constraints and orientational disorder in the tetraphenylporphyrin aggregates determine the luminescence yield relative to the monomeric species. The cofacial arrangement of the macrocycles in phthalocyanine aggregates results in a forbidden S_1–S_0 transition and thus in a complete disappearance of the luminescence.

Molecular electronics, photonics and iono-electronics are currently receiving great interest. A lot of ongoing research deals with the construction of nanometre-sized, self-organizing systems capable of transporting electrons, holes, excitons and/or ions. The combination of electronic and ionic transport processes in supramolecular devices could be of great importance in the development of future nano-electronic devices.

In this respect, molecular assemblies of porphyrins and phthalocyanines (Pcs) have been the subject of intensive research in view of their fascinating electronic and optical properties. The spontaneous arrangement of large aromatic macrocycles is facilitated by peripheral substitution with long alkyl or alkoxy chains. For several porphyrins[1–2] and phthalocyanines,[3–8] discotic thermotropic mesomorphic behaviour was observed, resulting in long linear stacks of aromatic moieties surrounded by insulating hydrocarbons, which might enhance the one-dimensional nature of electronic transport processes.[9–11]

Recently, it has been found that introduction of hydrophilic groups at the peripheral sites of the Pcs results in the formation of lyotropic mesophases. For example, attachment of oligo(ethylene oxide) moieties results in columnar lyotropic mesophases in addition to thermotropic columnar phases.[12–13] Furthermore, the attachment of polar side chains such as oligo(ethylene oxide) moieties and crown ether rings to large aromatic macrocycles is also of interest in the construction of supramolecular wires and ion conducting channels.[4,13a] Several porphyrins and phthalocyanines of these types have been designed in order to investigate complexation behaviour and the potential for electronic and ionic conduction.[14–19]

In our efforts to construct molecular assemblies which combine the functions of electronic and ionic conduction, we have recently reported[20] the thermotropic phase behaviour and aggregation properties of a series of tetraphenylporphyrin (TPP) derivatives in which the TPP macrocycle and a polar ethylene oxide part are separated by isolating hydrocarbon spacers (*e.g.* TPP **1**). It appeared that these compounds do not show mesomorphic behaviour but they tend to organize into similar and ordered J-type aggregates in solution, at the air–water interface and on solid substrates.

In this paper we describe the synthesis, thermotropic behaviour and self-organizing properties of three structurally related tetraphenylporphyrins (**1–3**) and two phthalocyanine compounds **4a,4b**. In the TPPs **1** and **2** the polar units and the TPP cores are separated by an alkoxy and an alkyl spacer, respectively. This was done since it has been found that the presence of ether linkages in the side chains directly attached to the phenyl substituent dramatically affects the thermotropic phase behaviour.[2] In TPP **3**, which is an isomer of **2**, the sequence of the polar and non-polar parts is inverted. Pcs **4a** and **4b** contain side-chains which are identical to those of TPP **1**; they are designed in order to compare the physicochemical behaviour of TPP and Pc-aggregates. The self-assembling features of these compounds have been studied by optical spectroscopic methods (absorption, fluorescence).

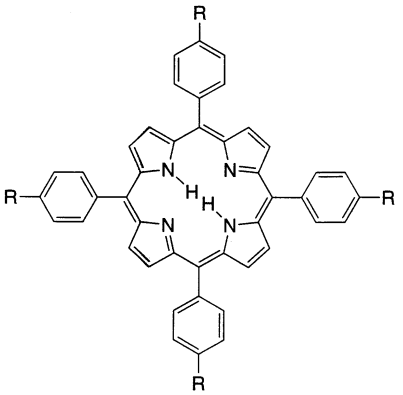

1 R = $O(CH_2)_6O(C_2H_4O)_3Me$

2 R = $(CH_2)_5O(C_2H_4O)_3Me$

3 R = $O(C_2H_4O)_3C_6H_{13}$

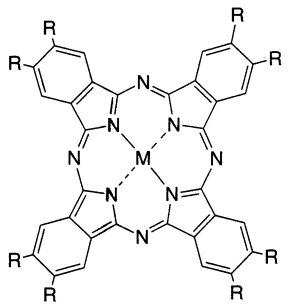

4a M = H_2
b M = Cu

R = $O(CH_2)_6O(C_2H_4O)_3Me$

Results

Synthesis

TPP **1** was synthesized as described previously.[20]

The synthetic procedure for the TPPs **2,3** and Pcs **4a,b** is presented in Scheme 1 and 2.

5-Phenyl-1-hydroxypentane was brominated using PBr_3. Substitution of the bromine by triethylene glycol monomethyl ether was carried out in the presence of sodium. An aldehyde group was introduced by adding hexamethylenetetraamine (HMTA) in trifluoroacetic acid (TFA).[21]

TPP **2** was synthesized using the Adler method[22] by refluxing the substituted benzaldehyde and pyrrole in propionic acid.

The benzaldehyde, leading to TPP **3**, was synthesized as follows.

The hydroxy group in triethylene glycol monohexyl ether was replaced by chlorine using thionyl chloride. 4-Hydroxybenzaldehyde was then substituted by the chloro-derivative in the presence of a base and potassium iodide.

The steps leading to Pc **4a**, were carried out using known procedures[23] (Scheme 3). Bromination of catechol using molecular bromine, alkylation of dibromocatechol in the presence

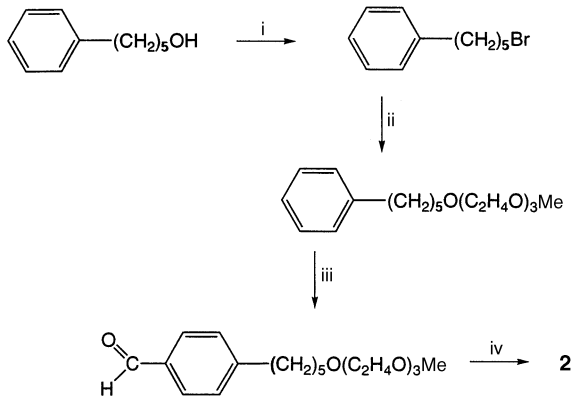

Scheme 1 *Reagents*: i, PBr_3; ii, $HO(C_2H_4O)_3Me$, Na; iii, HMTA, CF_3CO_2H; iv, pyrrole, propionic acid

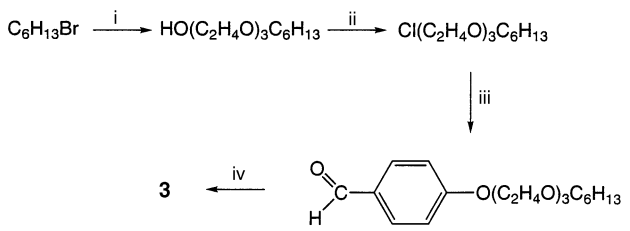

Scheme 2 *Reagents*: i, $HO(C_2H_4O)_3H$, Na; ii, $SOCl_2$; iii, 4-hydroxybenzaldehyde, K_2CO_3, butanone, KI; iv, pyrrole, propionic acid

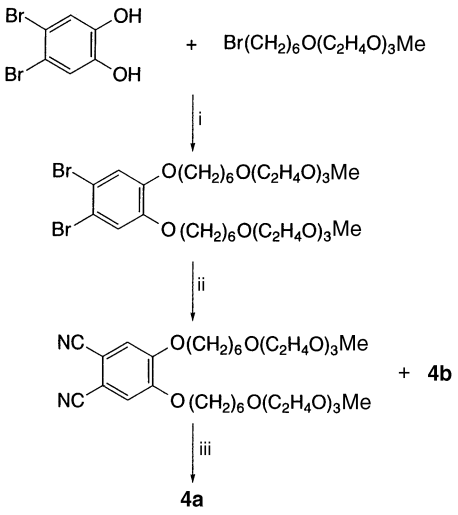

Scheme 3 *Reagents*: i, K_2CO_3, DMF; ii, CuCN, DMF; iii, DBN, EtOH

of base, a Rosenmund-von Braun reaction yielding the dicyanides and the conversion of the phthalodinitrile into **4a** by refluxing in absolute ethanol in the presence of DBN (1,5-diazabicyclo[4.3.0]non-5-ene). During the preparation of the dicyanides a substantial amount of **4b** was formed.

Thermotropic phase behaviour

Porphyrins. The phase transition temperatures as determined by differential scanning calorimetry (DSC) and polarization microscopy of the compounds **1–4** are compiled in Table 1.

The calorimetric data for TPP **1** have already been reported[20] and are included in Table 1. Upon heating from −50 °C, a phase transition with a small enthalpy change has been found at −22 °C (2.1 kJ mol^{-1}). Melting to the isotropic phase (clearing point) occurred at 67 °C (37 kJ mol^{-1}). The transitions have found to be reversible although some hysteresis occurred during the cooling cycle.

For TPP **2** no distinct transitions were observed with DSC during the first heating cycle starting at −40 °C but a broad endothermic transition centred at *ca.* 75 °C (*ca.* 23 kJ mol^{-1}) which corresponds to the clearing temperature. Subsequent cooling to −60 °C revealed no phase transitions. However, polarization microscopy showed the appearance of an anisotropic texture at 60–50 °C upon cooling from the isotropic phase.

In the case of TPP **3** a complex phase behaviour was observed. During the first heating three transitions have been found at −1, 30 and 47 °C, while isotropization occurred at 55 °C. Large hysteresis effects were observed during the first cooling cycle. In the second heating cycle two transitions (0 and 41 °C) have been observed before isotropization occurred. Inspection of this sample by polarization microscopy showed that during the heating no textural changes could be detected by passing through the lower phase transition temperatures. Upon cooling from the isotropic phase the material becomes anisotropic between 30 and 40 °C.

Phthalocyanines. Both Pcs **4a,b** are viscous oils at room temperature. During the first heating cycle of these compounds from room temperature to higher temperatures no phase transitions have been observed. Subsequent cooling to −50 °C shows an exothermic peak at −20 °C ($\Delta H = 21$ kJ mol^{-1}) for **4a**. A second heating cycle from −50 °C shows a broad exothermic peak at −20 °C ($\Delta H = 21$ kJ mol^{-1}) and an endothermic peak centred at *ca.* 5 °C ($\Delta H = 42$ kJ mol^{-1}).

The clearing temperatures, which were not observed with DSC, could be determined with polarization microscopy. The absence of the DSC peaks could probably be explained by the

Table 1 Phase transition temperatures (°C) and enthalpy changes ΔH (kJ mol^{-1}) (between brackets) for the investigated compounds **1–4**

compound	second heating cycle	first cooling cycle
1	C_1 −22 (2.1) C_2 67 (37) I	I 50 C_2 −40 C_1
2	C 70–75 (23) I	I 60–50 C[b]
3	C_1 0 (18) C_2 41 (24) C_3 55 (10) I	I 40–30[a] C_2 −10 C_1
4a	C[c] −20 (−21), 5 (42) D_{ho} 140–160[b] I	I 160–140[b] D_{ho} −20 (−21) C[c]
4b	D_{ho} 210–225[b] I	I 220–210[b] D_{ho}

[a]C is the crystalline phase, D_{ho} the hexagonal ordered discotic phase and I the isotropic phase. [b]These temperatures are determined with polarization microscopy, since DSC revealed no transitions. [c]C: partly crystallized, see text.

fact that the temperature range for isotropization for both Pcs is rather broad, 140–160 °C for **4a** and 210–225 °C for **4b**. A mosaic texture appears upon heating the compounds from room temperature until just before the clearing temperature (Plate 1). After cooling the isotropic melt there is a strong tendency to homeotropic alignment, except at the birefringent defects which appear as intense linear lines in the dark background (Plate 2). Between parallel analyser and polarizer digitate stars are observed (see Plate 3).

Aggregation in solution: UV–VIS absorption spectroscopy

Porphyrins. The presence of the polar ethylene oxide units in the hydrophobic side chains of the TPPs results in an increased solubility in polar solvents like acetone and methanol. For the investigated TPPs **1–3** it was found that they exist as monomers in these solvents at concentrations of 10^{-7}–10^{-4} M as they show a strong Soret or B-absorption band centred at *ca.* 420 nm and four characteristic Q-bands at 500–650 nm.

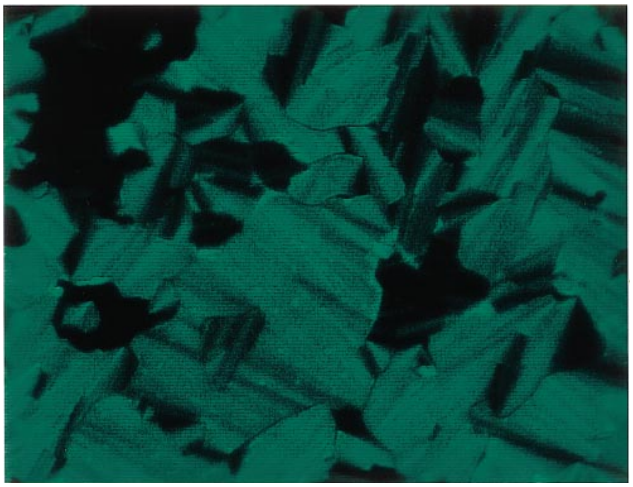

Plate 1 Micrograph of the mesophase of **4a** at 130 °C (crossed polarizers)

Plate 2 Micrograph of the mesophase of **4b** at room temperature after cooling from the isotropic phase (crossed polarizers)

Plate 3 Digitate stars observed in the mesophase of **4a** at 85 °C upon cooling from the isotropic phase (parallel polarizers)

For TPP **1**, it has recently been found[20] that in binary acetone–water mixtures aggregation of the TPPs into ordered aggregates was induced by increasing the volume fraction of water. The volume fraction at which aggregation occurs depends on the porphyrin concentration.

In this section we report on the aggregation properties of the TPPs **1–3** in methanol–water (v/v 1/1) and in pure water at concentrations of 10^{-5}–10^{-6} M.

The spectra of **1–3** in a number of solvents are shown in Fig. 1 for the Soret band region at a concentration of 5×10^{-6} M. The three strucurally related TPPs display rather different aggregation behaviour in aqueous media. In Fig. 1(*a*), it can be seen that in methanol, **1** is present as a monomer as it shows an intense Soret band at 418 nm ($\varepsilon = 4.5 \times 10^5$ dm^3 mol^{-1} cm^{-1}, FWHM = 750 cm^{-1}). However, a relatively broad red-shifted aborption band (FWHM = 2080 cm^{-1}) is found at 428 nm directly after addition of 15 μl 1 mM acetone solution of **1** into 3 ml of water. After several hours, this broad band splits into a relatively intense band at 440 nm ($\varepsilon = 3.3 \times 10^5$ dm^3 mol^{-1} cm^{-1}, FWHM = 540 cm^{-1}) and a relatively weak band at 400 nm ($\varepsilon = 7 \times 10^4$ dm^3 mol^{-1} cm^{-1}). The aggregation process is accelerated considerably, upon addition of a non-ionic amphiphile, polyoxyethylene(23) lauryl ether (CMC = 6–9 × 10^{-5} M, abbreviated as $C_{12}E_{23}$). The spontaneous formation of aggregates was indicated by similar changes in the optical spectrum as in the former case ($\varepsilon_{440} = 5 \times 10^5$ dm^3 mol^{-1} cm^{-1}, FWHM = 250 cm^{-1}).

In Fig. 1(*b*), it is shown that in methanol–water (v/v 1/1) a broad, asymmetric absorption band is initially found at 430 nm. In this solvent mixture, spontaneous aggregation is thus hindered. The aggregation process can again be accelerated by addition of $C_{12}E_{23}$, resulting in the same spectral features as observed for **1** in water. However, in contrast to pure water the aggregates are not stable in methanol–water, since the

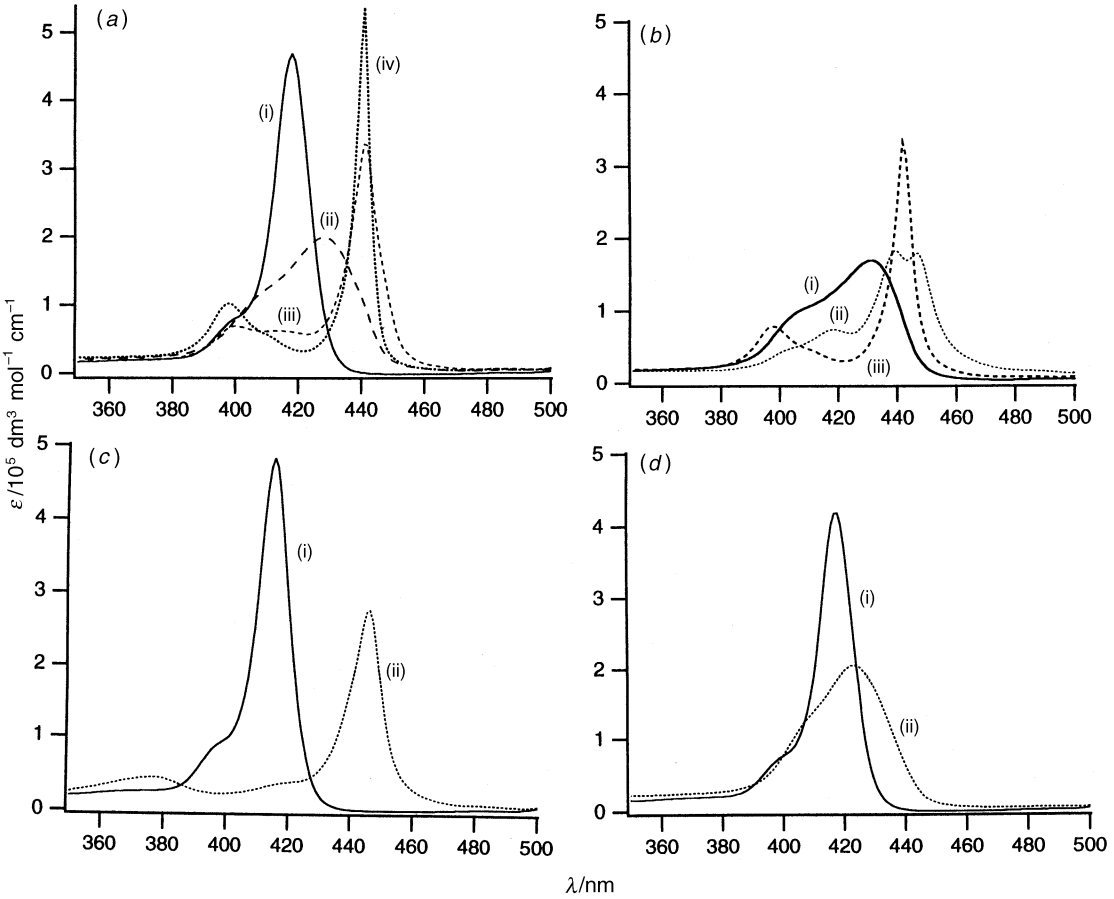

Fig. 1 Visible absorption spectra of (*a*) TPP **1** in (i) MeOH, (ii) H_2O (+0.5% acetone) directly after preparation of the solution, (iii) H_2O (+0.5% acetone) after 3 h, (iv) after addition of $C_{12}E_{23}$; (*b*) TPP **1** in (i) MeOH–H_2O (1:1 v/v) directly after preparation of the solution, (ii) after addition of $C_{12}E_{23}$, (iii) after 1 d; (*c*) TPP **2** in (i) MeOH, (ii) H_2O; (*d*) TPP **3** in (i) MeOH, (ii) H_2O. Measurements were performed at room temperature (concentration: 5×10^{-6} M).

spectrum changes into a split band centred at 440 nm while the blue-shifted band disappears.

For TPP **2**, spontaneous aggregation is found in water [Fig. 1(*c*)]. The spectral features of these aggregates are somewhat different from those of **1** in water. The red-shifted band is now located at 446 nm ($\varepsilon = 2.8 \times 10^5$ dm^3 mol^{-1} cm^{-1}) and somewhat broader (FWHM = 600 cm^{-1} *cf.* 250–500 cm^{-1} for **1**). Moreover, an additional band appears at the blue side (375 nm) of the spectrum. Addition of $C_{12}E_{23}$ does not have any significant effect on the spectral behaviour. Identical spectral behaviour was observed in a methanol–water (v/v 1/1) mixture (spectra not shown).

The spectrum of TPP **3** in pure water is characterized by a relatively broad absorption band (FWHM = 1800 cm^{-1}) centred at *ca.* 425 nm directly after preparation of the solution. This is shown in Fig. 1(*d*) together with the monomeric spectrum of **3** in methanol. In addition, the spectrum in methanol–water (v/v 1/1) is essentially the same (not shown). No further red-shift and sharpening of the bands were observed on a longer timescale.

Phthalocyanines. Both Pcs are highly soluble in a large variety of solvents except for alkanes like pentane and hexane.

The optical absorption spectra of **4a** and **4b** were measured in a range of solvents and are displayed in Fig. 2(*a*) for **4a**; **4a** shows two intense Q_x and Q_y bands at 660 ($\varepsilon = 1.25 \times 10^5$ dm^3 mol^{-1} cm^{-1}) and 700 nm ($\varepsilon = 1.6 \times 10^5$ dm^3 mol^{-1} cm^{-1}) in chloroform, while for **4b** one intense Q-band at 680 nm ($\varepsilon = 2 \times 10^5$ dm^3 mol^{-1} cm^{-1}) is observed (spectrum not shown). These bands are characteristic for the monomeric species. In water, the spectrum is blue-shifted and broadened. The maximum of the Q-band is located at 620 nm with an extinction coefficient of 2×10^4 dm^3 mol^{-1} cm^{-1}. This spectral behaviour is characteristic of columnar aggregated Pcs.[5b] It can also be seen in Fig. 2(*a*), that the spectrum in methanol contains a minor contribution of the monomeric species as was indicated by the weak shoulders at 660 and 770 nm. It should be noted that for **4b**, the spectral behaviour is essentially the same (spectra not shown).

The tendency of the Pcs **4a** and **b** to form aggregates increases in the order toluene ($\varepsilon_r = 2.4$), chloroform ($\varepsilon_r = 4.8$) < acetone ($\varepsilon_r = 21$) < acetonitrile ($\varepsilon_r = 37$) < ethanol ($\varepsilon_r = 24$) < methanol ($\varepsilon_r = 34$) < water ($\varepsilon_r = 80$), indicating that aggregation of the Pcs is not facilitated simply by increasing the bulk relative permittivity (ε_r). This is further confirmed by the fact that in an apolar solvent, such as pentane ($\varepsilon_r = 1.8$), aggregation also occurs already at very low concentrations.

Aggregation in solution: fluorescence spectroscopy

Porphyrins. The fluorescence characteristics of the TPPs **1–3** are compiled in Table 2.

For **1** in water, it was found that directly after preparation of the solution, the fluorescence is quenched by *ca.* 75% relative to the monomeric species in methanol. Addition of $C_{12}E_{23}$ leads to a twofold enhancement of the quantum yield and a small blue shift of the fluorescence bands.

For TPP **2**, spontaneous aggregation occurs in methanol–water (v/v: 1/1) and water (see former section). In methanol–water a small decrease of the quantum yield has been found as compared to the monomer in pure methanol, while in water a 70% reduction of the fluorescence yield was observed.

It was also shown in the former section that no spontaneous aggregation occurred for TPP **3** in water and methanol–water.

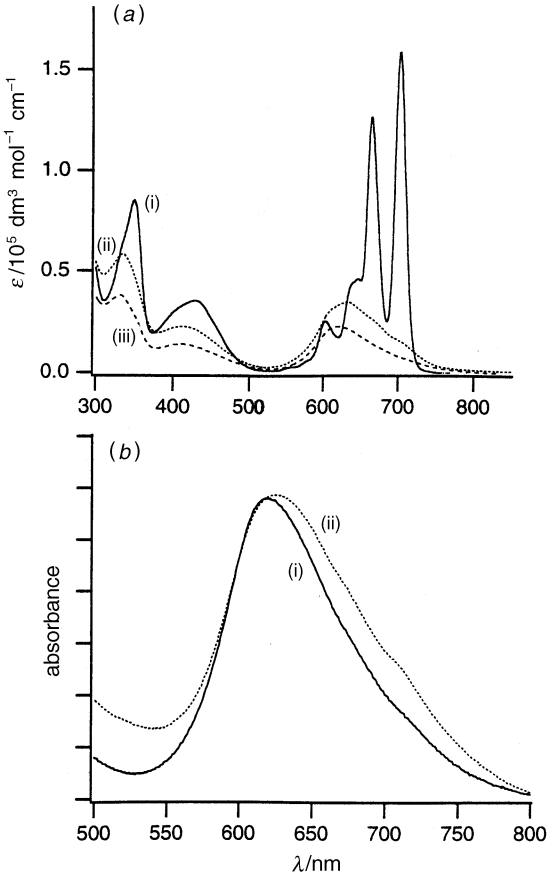

Fig. 2 Visible absorption spectra of **4a** (*a*) in (i) $CHCl_3$, (ii) MeOH and (iii) H_2O at room temperature (concentration: 5×10^{-6} M) and (*b*) in (i) H_2O and (ii) of spin-coated film on a glass substrate

This resulted in lower luminescence yields of resp. 0.13 and 0.18 *vs.* methanol (see Table 2).

Phthalocyanines. For **4a**, monomeric Q-emission bands are observed in chloroform at 710 and 790 nm. The fluorescence yield of the Pc is 3–4 times higher than for the TPPs. In methanol, a weak fluorescence is observed which is attributed to residual monomeric Pcs in the solution as was confirmed by fluorescence excitation spectra. In water the luminescence is totally quenched. No emission is observed for **4b** since luminescence comes from a tripdoublet state with a very low quantum yield at room temperature.[24]

Discussion

Thermotropic phase behaviour

The calorimetric data of the investigated TPPs show that incorporation of the ethylene oxide fragments in the side chains markedly affects the phase behaviour compared to appropriate reference compounds such as linear alkoxy and alkyl phenyl porphyrins. If **1** is compared with tetrahexadecyloxyporphyrin ($R = OC_{16}H_{33}$), which has a chain of comparable length (17 *cf.* 18 atoms),[20] a decrease of 51 °C of the clearing temperature is observed. An even more remarkable difference in phase behaviour is observed if **2** (side chain contains 16 atoms) is compared with tetra(hexadecylphenyl)porphyrin ($R = C_{16}H_{33}$). The latter TPP exhibits two phases between the crystal and isotropic phase which were assigned to be discotic lamellar (D_L) mesophases.[2] The clearing temperature has been found at 129 °C which is *ca.* 55 °C higher than for **2**.

For Pc **4a** a similar comparison can be made. For $H_2Pc[OC_{18}]_8$ ($R = OC_{18}H_{37}$), it has been reported[9b] that a $C \rightarrow D_h$ transition occurs at 98 °C ($\Delta H = 239$ kJ mol^{-1}) while the clearing temperature has been found at 247 °C ($\Delta H = 18$ kJ mol^{-1}). The clearing temperature for **4a** is considerably lower and found between 140 and 160 °C.

The mosaic textures which are observed for **4a** (Plate 1) and the digitate stars between parallel analyser and polariser (Plate 3) are indicative of a hexagonal discotic columnar mesophase.[6a–c] Similar textures were earlier observed for $H_2Pc[OC_{12}]_8$ ($R = OC_{12}H_{25}$) and the nature of the columnar phase of the latter compound was identified as a discotic hexagonal ordered mesophase D_{ho} by means of X-ray diffraction analysis. We conclude therefore that **4a** displays a D_{ho} mesophase.

From our DSC data, we cannot make a definite conclusion about the nature of the phase transitions between −20 and +5 °C. The observed exothermic peaks at −20 °C during cooling and subsequent heating can be due to a strongly retarded crystallization of the side-chains because of the disordered ethylene oxide units, while the endothermic peak at 5 °C can be attributed to melting of the side-chains. Detailed X-ray diffraction analysis, however, should be used to identify these transitions. It is apparent, however, that by introduction of the ethylene oxide units, it is possible to reduce the $C \rightarrow D_h$ transition temperature to such an extent that a columnar mesophase is observed even at room temperature. Comparable phase behaviour has recently been found by Clarkson for octa-substituted Pcs containing a combination of oligo(ethylene oxide) and alkyl substituents.[13a]

Finally, we come to the conclusion that liquid crystalline behaviour is only observed for the Pcs while the investigated TPPs are all non-mesomorphic. The presence of the mesophenyl groups, which are twisted with respect to the porphyrin core[25,26] prevents a close packing of the rings resulting in direct melting from the solid to the isotropic phase. Phthalocyanines, however, show very strong stacking of the flat rings, so that columnar order is preserved during melting of the side chains. The substitution of the alkyl or alkoxy chains with ethylene oxide units leads to more conformational disorder in the side chains, which results in a marked reduction of the melting and clearing temperatures.

Aggregation in solution: UV–VIS absorption spectra

Theory. The large spectral changes which occur upon aggregation are generally interpreted by the molecular exciton

Table 2 Relative fluorescence yields[a] and wavelength maxima [in brackets, nm] of the porphyrins **1–3** in solution at room temp.

solvent	**1** $I/I_{methanol}$ (λ_{max}/nm)	**2** $I/I_{methanol}$ (λ_{max}/nm)	**3** $I/I_{methanol}$ (λ_{max}/nm)
chloroform	0.94 [659, 724]	0.95 [654, 720]	1 [657, 723]
methanol	1 [656, 721]	1 [651, 717]	1 [655, 721]
methanol–water (1 : 1 v/v)	0.48 [657, 723]	0.70 [653, 721]	0.18 [659, 725]
water[b]	0.25 [655, 719]	0.33 [653, 721]	0.13 [659, 725]
water (+$C_{12}E_{23}$)[c]	0.50 [651, 717]		

[a]The yields *I* are relative to the yields measured in methanol. Excitation was performed at 515 nm (concentration = 5×10^{-6} M). [b]Direct after preparation of the solution and degassing. [c]After addition of excess of $C_{12}E_{23}$.

approximation developed by Kasha.[27] This model, which neglects electronic overlap of the π-systems, is based on the interaction between localized transition dipole moments. The coupling results in a splitting of the monomer state into a higher energy and a lower energy contribution. The resulting transition energy ($E^{\pm}$) is related to the energy of the monomer, E° eqn. (1)

$$E^{\pm} = E^{\circ} + D \pm V \quad (1)$$

in which D is a dispersion energy term and reflects the change in environment from monomer to oligomer, while V is the exciton splitting energy. For a cofacial array of N chromophoric units this term is related to the magnitude of the transition moment (M) and the geometry of the aggregate as given by eqn. (2).

$$V \approx 2\left\langle \left(\frac{N-1}{N}\right)\frac{M^2}{R^3}(1-3\cos^2\alpha)\right\rangle \quad (2)$$

In eqn. (2), R is the centre-to-centre distance of two chromophores in the aggregate and α is the angle between the centre-to-centre vector and the transition moment, which are assumed to be parallel in this case. The theory predicts, from the selection rule, that when $\alpha < 54.7^{\circ}$ the absorption band of the aggregate will be red-shifted and when $\alpha > 54.7^{\circ}$, the band will be blue shifted.

The assembling number, N, in the stacks can be evaluated semiempirically by eliminating the unkwown variables in eqn. (2) which leads to eqn. (3)

$$1/N = 1 - [\Delta E(N)/\Delta E(N \rightarrow \infty)] \quad (3)$$

where $\Delta E(N)$ is the exciton shift with assembling number N and $\Delta E(N \rightarrow \infty)$ for an infinite stack. It can be seen from eqns. (1–3) that the energy shift doubles going from a dimer ($N = 2$) to extended aggregates ($N = \infty$).

Porphyrins. In the metal free-base TPPs, the intense Soret or B-band has two degenerate perpendicular transition dipole components x and y. The lowest excited state is split up into two components, giving the four characteristic Q_x (0–1), Q_x (0–0), Q_y (0–1), Q_y (0–0) absorptions. The largest energy shifts are observed in the Soret band region which is a direct indication of strong exciton coupling. The magnitude of transition moment M for the Q-bands is very low, as compared with the Soret band, and only minor shifts are observed in the spectra.

In the context of the exciton model we can qualitatively interpret the observed spectral changes of the aggregated TPPs relative to the monomers.

For TPP **1**, a broad Soret absorption band is found at 422 nm after injecting the acetone solution in 3 ml of water. If there is a strong variation of the mutual distance R and torsion angle between the transition moments, it will lead to substantial broadening of the absorption band. The spectral changes observed on a longer time scale are explained by an increasing interaction of the porphyrin rings (smaller R). The red-shifted peak is rather narrow as compared to the monomeric species and indicates a homogeneous environment of the macrocycles. The peaks sharpen even more when an excess of non-ionic surfactant is added. At these concentrations micelles of $C_{12}E_{23}$ are formed and the porphyrin aggregates are probably embedded in the hydrophobic part of the micelle resulting in more order and an enhanced stability of the aggregate.

The spontaneous aggregation of **1** in water into ordered assemblies is retarded since water molecules are able to interact with the oxygen atoms directly linked to the phenyl rings. In **2**, no oxygen atoms are linked to the phenyl groups, providing a clear separation of the hydrophobic macrocycles and the surrounding hydrophilic ethylene oxide groups. This separation results in a spontaneous formation of ordered aggregates as was indicated by a substantial red shift of the Soret band relative to the monomeric species. In **3**, the polar fragments are substituted directly at the phenyl ring. The strong interaction of the ethylene oxide fragments with water molecules prevents a close packing of the porphyrin macrocycles and hinders the formation of ordered assemblies.

In order to deduce a structural model for the arrangement of the porphyrin macrocycles, the absorption spectra can be interpreted in terms of a displacement along the x and y axes (Fig. 3).

For aggregates of **1**[20] and related tetraalkoxyphenyl porphyrins,[28–30] a splitting of the Soret band into a blue- and a red-shifted component relative to monomeric species has been observed. A stack-of-cards configuration has been proposed[28] in which the porphyrin macrocycles are oriented edge-on-edge with a separation distance of approximately 4–5 Å [Fig. 3]. The large difference in intensity between the two bands at 400 and 440 nm remains, however, unclear and cannot be explained by the exciton theory [see Fig. 1(*a*)].

In an alternative, symmetrical model, a head-to-tail type arrangement could be formulated in which the degenerated transition dipole moments give rise to one excitonic splitting[31] [Fig. 3(*d*)]. The high energy transition, which is normally forbidden in a parallel coplanar situation, gains some transition probability due to a small deviation of the parallel alignment of the transition dipole moments. This explains the presence of the low-intensity blue shifted band.

A similar phenomenon has been found in polymeric cofacially stacked O-linked Si-Pc$(OC_{12}H_{25})_8$ aggregates[6d] [see Fig. 3(*b*)]. The strong cofacial interaction of the Pc-macrocycles results in a blue shifted band of high intensity ($\alpha = 90^{\circ}$) and a weaker red-shifted band. This splitting might be indicative of a non-linear Si—O—Si angle, resulting in a deviation from zero of the S_0–S_1 transition moment.

For **2**, a larger red-shift of the Soret band has been found (446 nm) than for **1**, while a blue-shifted absorption band is centred at 375 nm. These features can be interpreted in a similar way as for **1**, so that the most plausible structural arrangement is head-to-tail with a small deviation of a parallel alignment of the transition dipoles. Minor structural differences in the aggregates exist, however, between **1** and **2** due to the presence of the ether linkages attached to the phenyl ring in **1**.

We have not performed experiments in order to determine the assembling number of the aggregates yet. In the literature, attempts have been made to calculate the aggregation number

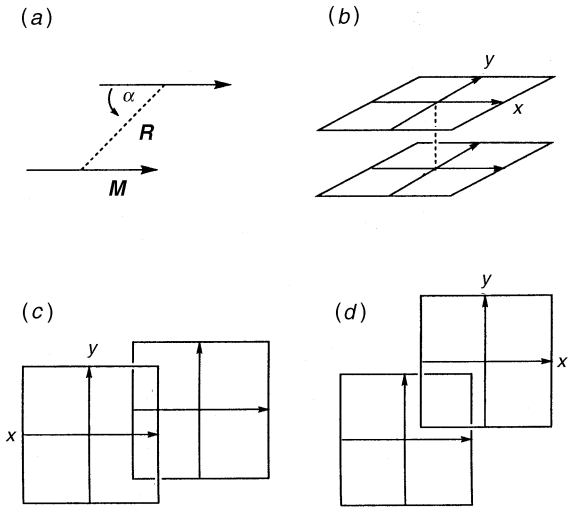

Fig. 3 Structural arrangements of porphyrins or phthalocyanines in aggregates (*a*) α the angle between the transition dipole moment (***M***) and the centre-to-centre vector (***R***), (*b*) face-to-face x,y: $\alpha = 90^{\circ}$, blue shift (side view), (*c*) edge-to-edge, x: $\alpha < 54.7^{\circ}$, y: $\alpha > 54.7^{\circ}$ red and blue shift (top view) and (*d*) head-to-tail, x,y: $\alpha < 54.7^{\circ}$ red shift (top view) [ref. 25(*b*)]

of stacks by means of fluorescence quenching studies. Different numbers for tetraalkoxyphenylporphyrin assemblies have been extracted for domain aggregates in LB-films ($N \geqslant 7$)[28] and aggregates in vesicles ($N \approx 4$).[29] The reported maxima (400 and 440 nm) in the absorption spectrum for these TPP aggregates are, however, identical despite of the different aggregation number. Interestingly, a dilute aqueous solution of **1** displays an identical absorption spectrum. It is expected that the solution consists mainly of dimers. Upon increasing the concentration no spectral changes are observed. Furthermore, the absorption spectrum of a spin-coated film has been found to be the same as that of an aqueous solution.[20] It is expected that larger aggregates are formed in solid films, although the film could consist of repeating aggregates of dimers and trimers.

The exciton model predicts an increasing energy shift with increasing assembling number [eqns. (2) and (3)]. The absorption spectra of aggregated tetraalkoxyphenyl porphyrins derivatives seem to be identical, irrespective of the different assembling numbers of the stacks. It is not exactly clear why the exciton approximation cannot be applied in this particular case, or the numbers extracted from the fluorescence quenching studies are incorrect. It seems useful to have a polymeric array of TPP molecules in order to determine $\Delta E(N \rightarrow \infty)$, while more direct methods for the determination of aggregation number are recommended.

Phthalocyanines. The lowest excited state of a mononuclear metal-free Pc is split into two components Q_x and Q_y, giving two main sharp absorptions at 660 and 700 nm. In a metallo-Pc (*e.g.* **4b**) the excited state is doubly degenerate, giving rise to one absorption band at 680 nm. Upon aggregation, the Q-states split into a higher and a lower energy contribution.

From the absorption spectra in Fig. 1 and 2, it becomes clear that the tendency for aggregation of the Pcs **4a/b** is larger as compared to the TPPs **1–3**. This difference can be explained by a larger π-system for the Pcs, resulting in a stronger π–π interaction of the aromatic rings, while the flatness of the Pc-core provides for a closer packing of the rings.

It has already been pointed out by Schutte[32] that aggregation in polar solvents is caused by the fact that there is a strong solvent–solvent interaction excluding the Pc molecules from solution which causes them to aggregate. This explains the fact that aggregation in methanol is stronger than in acetonitrile, despite the higher relative permittivity for acetonitrile ($\varepsilon_{\text{methanol}} = 34$ *vs.* $\varepsilon_{\text{acetonitrile}} = 37$), since there is a much stronger tendency for hydrogen bond formation in methanol. The aggregation effect in solvents with low relative permittivities (*e.g.* pentane) is explained by minimization of the screening of the Pc–Pc interaction.

In contrast to the TPPs described above, which form typically head-to-tail type of aggregates, the Pcs display a broad blue-shifted absorption band as compared to the monomer case. This is indicative of the formation of face-to-face or H-type of aggregates in which the rings are cofacially stacked (Fig. 3(*b*)]. The maximum of the absorption band lies at approximately 620 nm. In other studies of Pc-aggregates,[32,33] it has been found that assembling numbers could succesfully be calculated by using the modified exciton theory [eqn. (3)]. Dimers of Pcs octasubstituted by branched alkoxy chains[32] or crown ethers[15a] display energy shifts which are identical as for the aggregates of **4a** in water. For the latter species, the mutual distance, R, as well as the other parameters in the exciton approximation, M and α, are expected to be similar to those reported for the former Pc dimers. Thus, we come to the conclusion that in a dilute solution ($c = 5 \times 10^{-6}$ M), **4a** mainly consists of dimers. The absorption spectrum of a spin-coated film of **4a** [Fig. 2(*b*)] display the same wavelength maximum as for water ($\lambda_{\max} = 620$ nm) suggesting that the film consists of an assembly of dimers [Fig. 3(*b*)].[34]

Aggregation in solution: fluorescence spectroscopy

The different fluorescence properties of the TPP aggregates as compared to the Pc-aggregates can be understood in the framework of the exciton theory and is schematically depicted in Fig. 4. It has been demonstrated that large exciton coupling occurs in the Soret band of the TPPs while relatively minor coupling effects were observed in the Q-bands. In general, fluorescence from TPPs in solution occurs primarily from the Q-state (S_1), although B-state (S_2) fluorescence has been observed for some monolayer assemblies.[26] Q-State fluorescence in TPP aggregates is thus in principle an allowed transition from a relatively unperturbed Q-state [Fig. 4(*a*)].

It has often been stressed that the fluorescence of aggregates is quenched relative to monomeric species as a result of interchromophoric interactions[35,36] but in other studies[1b,37] it has been found that the fluorescence quantum yields in porphyrin dimers or solid films could be as high as for the monomers. Important factors that determine the competition of internal conversion and radiative decay are the steric geometry and the orientational order of the aggregates.[1b,17]

The fluorescence data presented in this paper reveal a reduction of the fluorescence yield for all the TPPs relative to the monomers indicating that a significant amount of self-quenching occurs in the aggregates. The lowest fluorescence yields were found in water for the TPPs **1** directly after preparation of the solution and for **3** in water and methanol–water (v/v 1/1). The UV–VIS spectra displayed relatively broad Soret bands which are explained by the existence of aggregates with an inhomogeneous environment. The orientational disorder results in enhanced rates of internal conversion thereby diminishing the fluorescence quantum yield. Interestingly, addition of $C_{12}E_{23}$ leads to well-ordered aggregates (see Plate 1) and an enhancement of the fluorescence yield. Moreover, **2** forms ordered aggregates in methanol–water of which the fluorescence yield has been found to be nearly identical to that of the monomer. This supports our interpretation that the fluorescence yields of TPP aggregates are strongly determined by the degree of orientational order in the aggregates.

The situation for the Pcs is reversed as compared to the TPPs [Fig. 4(*b*)], supported by the spectral shifts upon aggregation, which are in the opposite direction to those for the TPPs. The strongest coupling now occurs in the Q-band region where the transition probability is larger than in the Soret band region. Since the lowest energy transition is formally

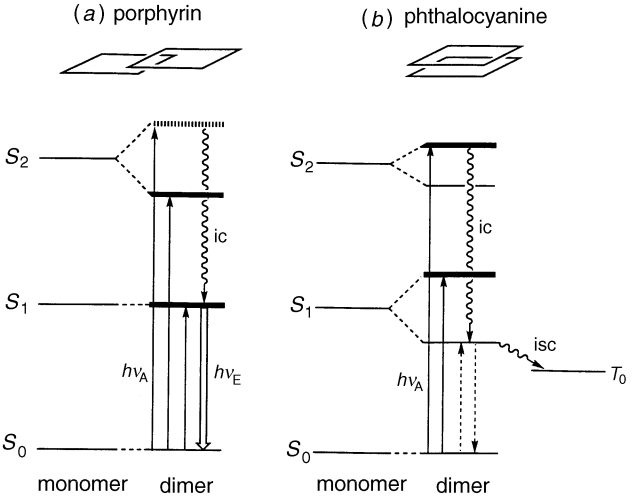

Fig. 4 Schematic representation of the relative energy levels for (*a*) a head-to-tail type of porphyrin dimer and (*b*) a H- or cofacially stacked dimer. $h\nu_A$ Refers to allowed absorptions to higher levels (plain arrows), $h\nu_E$ is the dimer fluorescence (open arrow), ic = internal conversion, isc = intersystem crossing and the dashed arrows represent forbidden radiative transitions.

forbidden in cofacially arranged (H-) aggregates no fluorescence and an enhanced intersystem crossing to triplet states is expected.[27b] This has indeed already been observed for Pc-dimers in solution[38] and for crown ether Pcs[16] which form perfectly eclipsed cofacial dimers in the presence of ions, resulting in a relatively narrow blue-shifted Q-band and complete disappearance of the fluorescence.

The relatively broad blue-shifted Q-band in our Pc-dimers indicates a more flexible mutual arrangement of the Pc-macrocycles in the aggregate resulting in a mixture of staggered and eclipsed dimers. In contrast to the TPP-aggregates, we conclude that it is not the disordered environment which explains the total quenching of the fluorescence in Pc-aggregates but can be fully interpreted in terms of the exciton approximation.

Luminescence studies have also been carried out for the discotic Pc[OC_{12}]$_8$ as a function of temperature.[39] At the solid-to-mesophase transition, a sharp drop in luminescence intensity occurred. This was explained in terms of a change in the rate of energy migration to quenching sites. However, the phase transition is accompanied by a structural change from a tilted to a cofacial arrangement of the macrocycles which in our opinion perfectly accounts for the disappearance of the fluorescence.

Finally, some Pcs have shown a high efficiency in photodynamic therapy since they absorb at longer wavelengths than TPPs, especially in a region where human tissues are transparent. In general, aggregation of Pcs leads to a reduction of the luminescence yield, which is a serious drawback in possible biological applications. It is therefore interesting that very recently a Pc has been synthesized[40] with anti-aggregative properties by introduction of 16 polyoxyethylene side chains at the periphery of the Pc core. This was the first example of a water-soluble, non-ionic Pc which exhibits fluorescence in aqueous media.[41]

Conclusions

We have reported upon the thermotropic phase behaviour and the aggregation properties of three tetraphenylporphyrin and two phthalocyanine derivatives containing oligo(ethylene oxide) hydrocarbon units. None of the TPPs was found to be mesomorphic while the Pcs display discotic phases at room temperature. The incorporation of ethylene oxide units at the side chains results in a remarkable lowering of the melting and clearing temperatures as compared to derivatives with unbranched linear alkyl chain derivatives of similar length.

The tendency of Pcs to aggregate in solution has been found to be stronger than for the TPPs. The stronger π–π interaction and the flatness of the aromatic cores in the Pcs cause them to aggregate more strongly than the TPPs. The presence of meso-phenyl groups prevents a close packing of the rings. The TPPs form J- or head-to-tail type of aggregates, while Pcs tend to organize into H- or cofacially stacked aggregates.

Despite the structural similarities of the investigated TPPs, they display a strikingly different aggregation behavior in water. The velocity of organization into ordered assemblies depends on the number of ether linkages substituted at the meso-phenyl group and increases in the order **3**<**1**<**2**.

The luminescence properties of the TPP and Pc aggregates can be explained on the basis of the exciton approximation. The degree of self-quenching in the TPP aggregates relative to monomeric species proved to be a function of steric geometry and orientational order. The cofacial arrangement of the rings in Pc-aggregates results in a forbidden S_1–S_0 transition and a complete disappearance of the luminescence.

Comparison of the solution spectra of the investigated compounds with the spectra of spincoated films have indicated that the films consist of a repeating number of small aggregates (dimers). For practical applications in terms of charge and energy migration it is important to construct films of highly ordered assemblies consisting of large aggregates. On the other hand, the mobility of ions through polar channels is found to be much higher in amorphous regions than in crystalline regions. These requirements seem to be partly fulfilled in the discotic phase of Pc **4a**, in which the columnar order is preserved while the hydrophilic ethylene oxide units are in a liquid-like state. It should be noted, however, that there is an increased positional disorder of the aromatic units in the discotic phase, resulting in less efficient exciton/charge transport.

Materials in which the discs are strictly confined to a one-dimensional spine surrounded by a liquid-like hydrocarbon mantle could be of great interest in the construction of molecular wires capable of transporting ions and electrons. Polymeric O-linked Si–Pc **4a** will be a promising candidate for combining the functions of efficient electronic and ionic conduction in one system and future research will be planned in order to design such materials.

Experimental Section

General methods

NMR spectra were acquired using a 200 MHz Bruker AC200 spectrometer at 298 K.

Differential scanning calorimetry (DSC) measurements were performed with a DSC 7 (Perkin Elmer) (heating/cooling rate 10 °C min^{-1}).

Melting points and textures were measured using a Mettler hot-stage attached to an Olympus polarizing microscope. Heating/cooling rates were 10 °C min^{-1} and near the transition temperatures 2 °C min^{-1}.

The electronic absorption spectra were recorded with a Perkin Elmer Lambda 18 spectrophotometer. Fluorescence spectra were recorded on a Perkin Elmer LS5. The aqueous solutions for absorption and fluorescence measurements were prepared by injecting a small volume (10–20 μl) of 1 mM solution of the compounds in acetone *via* a microsyringe into 3 ml solvent.

Fluorescence yields for the TPPs were measured relative to the monomeric TPPs in methanol. All solutions were made in 1 cm cuvettes with an absorption at the excitation wavelength below 0.2.

The relative yields were then calculated by using: Yield = $[(A_s I_u n^2)/A_u I_s n_0^2]$ where: u subscript refers to the TPP in the unknown solvent and s to the TPP in methanol. A is the absorbance at the excitation wavelength, I the integrated fluorescence intensity across the band and n, n_0 the refraction index of the unknown solvent and methanol.

Synthesis of tetraphenylporphyrins 2 and 3

Tetrakis-(6,9,12,15-tetraoxahexadecyl)phenylporphyrin (2). 5-Phenyl-1-hydroxypentane (24.0 g, 0.15 mol) was added carefully to 14 ml of PBr_3 in 15 min while cooling the solution. The mixture was stirred at 100 °C for 1.5 h and then poured onto ice. After extraction with dichloromethane, the organic fractions were washed with water and $NaHCO_3$ solution and dried on $MgSO_4$. Vacuum distillation yielded 20.5 g (62%) of 5-phenyl-1-bromopentane. Bp: 146–148 °C (14 mmHg).

Sodium (0.50 g, 22 mmol) was dissolved in 25 ml of triethylene glycol monomethyl ether at 100 °C and cooled to room temp. 5-Phenyl-1-bromopentane (4.54 g, 20 mmol) was then added and the mixture was stirred at 100 °C for 3 h. The reaction mixture was poured onto ice and extracted with diethyl ether. The organic fractions were washed with water and the solvent was evaporated under reduced pressure.

The crude product was purified on silica gel [eluent light petroleum (40–60)–ethylacetate 1 : 4] yielding 4.78 g (77%) of 6,9,12,15-tetraoxahexadecylbenzene.

A mixture of the latter compound (2.98 g, 9.6 mmol) with 15 ml of trifluoroacetic acid was stirred at room temperature and then 1.54 g (11 mmol) hexamethylenetetraamine (HMTA) was added. The resulting mixture was stirred overnight at 90 °C. After evaporation of trifluoroacetic acid the residue was dissolved in water and stirred for 1 h. A solution of Na_2CO_3 was added until pH = 8. The solution was extracted with dichloromethane. The organic fractions were washed with NaCl solution, dried over $MgSO_4$ and the solvent was evaporated under reduced pressure. The crude product was purified on silica gel (eluent ethyl acetate–dichloromethane 1:1) yielding 1.53 g (47%) of 4-(6,9,12,15-tetraoxahexadecyl)-benzaldehyde.

The title compound was then synthesized by refluxing a mixture of 1 equiv. of benzaldehyde together with 1 equiv. pyrrole in propionic acid for 0.5 h. After evaporation of the propionic acid, the crude mixture was purified on silica gel (eluent dichloromethane with gradual addition of methanol) and finally on Al_2O_3 (act.II), eluent dichloromethane with gradual addition of methanol, yielding of the desired TPP **2** in a yield of 10%. Elemental analysis, Found: C, 71.43; H, 8.42; N, 3.55%. $C_{92}H_{126}N_4O_{16}$ requires C, 71.56; H, 8.23; N, 3.63%. δ_H (200 MHz, $CDCl_3$): −2.76 (s, 2H), 1.5–2.0 (m, 24H), 2.96 (t, 8H), 3.37 (s, 12H), 3.5–3.7 (m, 68H), 7.55 (d, 8H), 8.11 (d, 8H), 8.86 (s, 8H). UV–VIS, λ_{max}/nm (log ε/dm^3 mol^{-1} cm^{-1}), $CHCl_3$: 421(5.68), 522 (4.25), 554 (4.01), 593 (3.75), 649 (3.76).

Tetrakis(1,4,7,11-tetraoxahexadecyl)phenylporphyrin (3). Sodium (14 g, 0.61 mol) was dissolved in 364 g of triethylene glycol (2.43 mol) at 100 °C and cooled to room temp. 100 g (0.61 mol) of 1-bromohexane was added and the mixture was stirred for 5 h at 200 °C. The mixture was poured into water (500 ml) and light petroleum bp 100–120 °C (400 ml) and heated to 70 °C. After separation of the water layer, the organic fraction was washed with hot water (3 × 100 ml) and the solvent was evaporated. Vacuum distillation yielded 62.4 g (44%) triethylene glycol monohexyl ether (bp 125–130 °C/0.1 mmHg).

A mixture of 58.5 g (0.25 mol) triethylene glycol monohexyl ether and 19.75 g of pyridine (0.25 mol) was stirred and cooled in ice. 44.6 g (0.38 mol) Thionyl chloride was slowly added and the solution was refluxed for 1.5 h. After cooling to room temp., the mixture was poured into ice–water. A 10% (m/m) NaCl solution was then added and the resulting mixture was extracted with diethyl ether. The organic layers were washed with 10% (m/m) NaCl solution, dried and evaporated to dryness. Vacuum distillation yielded 52.7 g (84%) of 1-chloro-(3,6,9-trioxa)pentadecane (bp 125–130 °C/0.1 mmHg).

1-Chloro-(3,6,9-trioxa)pentadecane (38.3 g, 0.15 mol), 4-hydroxybenzaldehyde (12.2 g, 0.1 mol), K_2CO_3 (27.6 g, 0.2 mol) and 5.0 g of potassium iodide were stirred in 200 ml butanone and refluxed for 3 d. The precipitate was filtered off and washed with dichloromethane. The filtrate was concentrated and a solution of 30 g $NaHSO_3$ in 63 ml of water and 38 ml of ethanol was added and the resulting mixture stirred for 2 h. Extraction was then carried out with diethyl ether and the organic fractions were washed with water, dried over $MgSO_4$ and evaporated under reduced pressure.

Yield 7.6 g (23%) of 4-(1,4,7,10-tetraoxahexadecyl)-benzaldehyde.

The title compound **3** was then synthesized in *ca.* 10% yield using the same procedure as described above. Elemental analysis, Found: C, 71.66; H, 8.53; N, 3.51%. $C_{92}H_{126}N_4O_{16}$ requires C, 71.56; H, 8.23; N, 3.63%. δ_H (200 MHz, $CDCl_3$), −2.70 (s, 2H), 0.9 (t, 12H), 1.3 (m, 24H), 1.62 (q, 8H), 3.50 (t, 8H), 3.7–3.9 (m, 32H), 4.0 (t, 8H), 4.36 (t, 8H), 7.25 (d, 8H), 8.10 (d, 8H), 8.89 (s, 8H). UV–VIS, λ_{max}/nm (log ε/dm^3 mol^{-1} cm^{-1}), $CHCl_3$: 422(5.66), 519 (4.19), 556 (4.01), 593 (3.67), 650 (3.74).

Synthesis of the phthalocyanines 4a,b

1,2-Bis(1,8,11,14,17-pentaoxaoctadecyl)-4,5-dibromobenzene. A mixture of 1,2-dibromocatechol (5 g, 18 mmol), 1-bromo-7,10,13,16-tetraoxaheptadecane, (13.1 g, 40 mmol) and K_2CO_3 (16 g, 116 mmol) in 200 ml of DMF was stirred and heated to 100 °C for 24 h and then poured into water and extracted with $CHCl_3$ (3 × 150 ml). The organic layers were washed with water (3 × 100 ml), dried with $MgSO_4$ and the solvent was evaporated to give a brownish oil. The crude product was purified on silica gel (0.04–0.063 mm; eluent ethyl acetate) yielding the title compound as a yellow oil (8.2 g, 60%). δ_H (200 MHz, $CDCl_3$), 1.40 (m, 8H), 1.55 (q, 4H), 1.75 (q, 4H), 3.34 (s, 6H), 3.4 (t, 4H), 3.6 (m, 24H), 3.89 (t, 4H), 7.02 (s, 2H). ν/cm^{-1} ($CHCl_3$) 650 Ar–Br.

1,2-Bis(1,8,11,14,17-pentaoxaoctadecyl)-4,5-dicyanobenzene. A mixture of the preceding compound (3.9 g, 5 mmol) and Cu^{I}CN (1.25 g, 15 mmol) in 50 ml of DMF was refluxed for 24 h under a nitrogen atmosphere. The cooled mixture was poured in 150 ml of aqueous ammonia (25%) and air was bubbled through the solution for 24 h. The desired dinitrile was extracted with dichloromethane–methanol (4/1). The green organic phase was washed with water and dried over $MgSO_4$. Chromatography (silica gel, eluent ethyl acetate–methanol, gradient 1–3%) afforded 1.8 g (55%) of the title compound. δ_H (200 MHz, $CDCl_3$), 1.50 (m, 8H), 1.58 (q, 4H), 1.90 (q, 4H), 3.38 (s, 6H), 3.50 (t, 4H), 3.6 (m, 24 H), 4.05 (t, 4H), 7.11 (s, 2H). ν/cm^{-1} ($CHCl_3$): 2210 (CN).

A residual green fraction was isolated by elution with ethyl acetate–methanol (1/1) and identified as the copper–phthalocyanine **4b** (70 mg). Elemental analysis, Found: C, 61.03; H, 8.52; N, 4.06%. $C_{136}H_{224}N_8O_{40}Cu$ requires C, 61.07; H, 8.44; N, 4.19%. UV–VIS, λ_{max}/nm (log ε/dm^3 mol^{-1} cm^{-1}), $CHCl_3$: 613(4.55), 680 (5.30).

2,3,9,10,16,17,23,24-Octa(1,8,11,14,17-pentaoxaoctadecyl) phthalocyanine (4a). The dinitrile (1.6 g, 2.5 mmol) and DBN (0.37 g, 2.5 mmol) were dissolved in 8 ml of absolute ethanol and refluxed for 48 h. The reaction mixture turned dark green. After evaparation of ethanol, the crude oil was chromatographed on silica gel (eluent ethyl acetate–methanol 2–10%), alumina (act.II/III, eluent 2% MeOH in CH_2Cl_2). The last impurities were removed by soxhlet extraction with light petroleum (60–80) yielding the green sticky phthalocyanine **4a** (200 mg, 10%). Elemental analysis, Found: C, 62.67; H, 8.85; N, 3.93%. $C_{136}H_{226}N_8O_{40}$ requires C, 62.50; H, 8.72; N, 4.29%. δ_H (200 MHz, $CDCl_3$): 1.5–1.8 (m, 8H), (q, 16H), 3.34 (s, 24H), 3.5–3.7 (m, 108H), 4.63 (t, 16H), 8.95 (s, 8H). UV–VIS: λ_{max}/nm (log ε/dm^3 mol^{-1} cm^{-1}) $CHCl_3$: 602 (4.41), 646 (sh, 4.67), 665 (5.11), 702 (5.21).

This work is supported financially by the Dutch Agency for Energy and Environment (Novem). We are indebted to A. van Veldhuizen for performing the NMR measurements.

References

1 (*a*) B. A. Gregg, M. A. Fox and A. J. Bard, *J. Am. Chem. Soc.*, 1989, **111**, 3024; (*b*) B. A. Gregg, M. A. Fox and A. J. Bard, *J. Phys. Chem.*, 1989, **93**, 4227.
2 Y. Shimizu, M. Miya, A. Nagata, K. Ohta, I. Yamamoto and S. Kusabayashi, *Liq. Cryst.*, 1993, **14**, 795.
3 (*a*) M. J. Cook, *J. Mater. Sci.: Mater. Electron.*, 1994, **5**, 117; (*b*) M. J. Cook, *Adv. Mater.*, 1995, **7**, 877; (*c*) G. C. Bryant, M. J. Cook, T. G. Ryan and A. J. Thorne, *Tetrahedron*, 1996, **52**, 809.
4 C. F. van Nostrum, S. J. Picken, A. J. Schouten and R. J. M. Nolte, *J. Am. Chem. Soc.*, 1995, **117**, 9957.
5 (*a*) C. Piechowski, J. Simon, A. Skoulios, D. Guillon and P. Weber, *J. Am. Chem. Soc.*, 1982, **104**, 5245; (*b*) C. Piechowski and J. Simon, *Nouv. J. Chim.*, 1985, **3**, 159; (*c*) P. Weber, D. Guillon and A. Skoulios, *Liq. Cryst.*, 1991, **9**, 369.

6 (*a*) J. F. van der Pol, E. Neeleman, J. W. Zwikker, R. J. M. Nolte and W. Drenth, *Recl. Trav. Chim. Pays-Bas*, 1988, **107**, 615; (*b*) J. F. van der Pol, W. Drenth, E. Neeleman, J. W. Zwikker, R. J. M. Nolte, J. Aerts, R. Visser and S. J. Picken, *Liq. Cryst*., 1989, **6**, 5779; (*c*) J. F. van der Pol, PhD Thesis, University of Utrecht, 1990; (*d*) J. F. van der Pol, J. W. Zwikker, J. M. Warman and M. P. de Haas, *Recl. Trav. Chim. Pays-Bas*, 1990, **109**, 208; (*e*) P. G. Schouten, J. F. van der Pol, J. W. Zwikker, W. Drenth and S. J. Picken, *Mol. Cryst. Liq. Cryst*., 1991, **195**, 291.

7 L.-K Chau, C. Arbour, G. E. Collins, K. W. Nebesny, P. A. Lee, C. D. England, N. R. Armstrong and B. A. Parkinson, *J. Phys. Chem*., 1993, **97**, 2690.

8 T. Komatsu, K. Ohta, T. Watanabe, H. Ikemoto, T. Fujimoto and I. Yamamoto, *J. Mater. Chem*., 1994, **4**, 537.

9 (*a*) P. G. Schouten, J. M. Warman, M. P. de Haas, M. A. Fox and H. Pan, *Nature,* 1991, **353,** 736; (*b*) P. G. Schouten, J. M. Warman, M. P. de Haas, C. F. van Nostrum, G. H. Gelinck, R. J. M. Nolte, J. W. Zwikker, M. K. Engel, M. Hanack, Y. H. Chang and W. T. Ford, *J. Am. Chem. Soc*., 1994, **116**, 6880; (*c*) P. G. Schouten, PhD Thesis, Delft University of Technology, 1994, ISBN 90-73861-22-5.

10 (*a*) B. Blanzat, C. Barthou, N. Tercier, J.-J. André and J. Simon, *J. Am. Chem. Soc*., 1987, **109**, 6193; (*b*) D. Markovitsi, I. Lécuyer and J. Simon, *J. Phys. Chem*., 1991, **95**, 3620.

11 M. Hanack and M. Lang, *Adv. Mater*., 1994, **6**, 819.

12 N. B. McKeown and J. Painter, *J. Mater. Chem*., 1994, **4**, 1153.

13 (*a*) G. J. Clarkson, N. B. McKeown and K. E. Treacher, *J. Chem. Soc., Perkin Trans. 1*, 1995, 1817; (*b*) G. J. Clarkson, B. M. Hassan, D. R. Maloney and N. B. McKeown, *Macromolecules*, 1996, **29**, 1584; (*c*) G. J. Clarkson, A. Cook, N. B. McKeown, K. E. Treacher and Z. Ali-Adib, *Macromolecules*, 1996, **29**, 913.

14 T. Toupance, V. Ahsen and J. Simon, *J. Am. Chem. Soc*., 1994, **116**, 5352.

15 (*a*) O. E. Sielcken, M. M. van Tilborg, M. F. M. Roks, R. Hendriks, W. Drenth and R. J. M. Nolte, *J. Am. Chem. Soc*., 1987, **109**, 4261; (*b*) O. E. Sielcken, J. Schram, R. J. M. Nolte and W. Drenth, *J. Chem. Soc., Chem. Commun*., 1988, 108; (*c*) O. E. Sielcken, H. C. A. van Lindert, W. Drenth, J. Schoonman, J. Schram and R. J. M. Nolte, *Ber. Bunsen-Ges. Phys. Chem.,* 1989, **93**, 702.

16 N. Kobayashi and A.B.P. Lever, *J. Am. Chem. Soc*., 1987, **109**, 7433.

17 V. Thanabal and V. Krishnan, *J. Am. Chem. Soc*., 1982, **104**, 3643.

18 (*a*) T. Aida, A. Tajemura, M. Fuse and S. Inoue, *J. Chem. Soc., Chem. Commun*., 1988, 391; (*b*) S. Inoue, in *Supramolecular assemblies, new developments in biofunctional chemistry*, ed. Y. Marakami, Mita Press, Tokyo, 1990, p. 9.

19 C. S. Velázquez, J. E. Hutchinson and R. W. Murray, *J. Am. Chem. Soc*., 1993, **115**, 7896.

20 J. M. Kroon, P. S. Schenkels, M. van Dijk and E. J. R. Sudhölter, *J. Mater. Chem*., 1995, **5**, 1309.

21 H. Nakai, M. Konno, S. Kosuge, S. Sakuyama, M. Toda, Y. Arai, T. Obata, N. Katsube, T. Miyamoto, T. Okegawa and A. Kawasaki, *J. Med. Chem*., 1988, **31**, 84.

22 (*a*) A. D. Adler, F. R. Longo and W. Shergalis, *J. Am. Chem. Soc*., 1964, **86**, 3145; (*b*) A. D. Adler, F. R. Longo, J. D. Finarelli, J. Goldmacher, J. Assour and J. Korsakoff, *J. Org. Chem*., 1967, **32**, 476.

23 C. C. Leznoff in *Phthalocyanines, Properties and Applications*, vol. 1, ed. C. C. Leznoff and A. B. P. Lever, VCH, New York, 1989, 6.

24 (*a*) D. Eastwood and M. Gouterman, *J. Mol. Spectrosc*., 1969, **30**, 437; (*b*) R. L. Ake and M. Gouterman, *Theor. Chim. Acta*, 1969, **15**, 20.

25 V. Mckee and G. A. Rodley, *Inorg. Chim. Acta*, 1988, **151**, 233.

26 C. K. Schauer, O. P. Anderson, S. S. Eaton and G. Eaton, *Inorg. Chem*., 1985, **24**, 4082.

27 (*a*) E. G. McRae and M. Kasha, *J. Chem. Phys.,* 1958, **28,** 721; (*b*) M. Kasha, H. R. Rawls and M. Ashraf El-Bayoumi, *Pure Appl. Chem*., 1965, **11**, 371.

28 G. A. Schick, I. C. Schreimann, R. W. Wagner, J. S. Lindsey and D. F. Bocian, *J. Am. Chem. Soc.,* 1989, **111**, 1344.

29 (*a*) J. H. van Esch, M. C. Feiters, A. M. Peters and R. J. M. Nolte, *J. Phys. Chem*., 1994, **98**, 5541; (*b*) A. P. H. J. Schenning, D. H. W. Hubert, M. C. Feiters and R. J. M. Nolte, *Langmuir*, 1996, **12**, 1572.

30 S. Kugimaya and M. Takemura, *Chem. Lett*., 1990, 1355.

31 J. M. Kroon, E. J. R. Sudhölter, J. Wienke, R. B. M. Koehorst, T. J. Savenije and T. J. Schaafsma, *Proc. 13th Eur. Photovoltaic Solar Energy Conf*., Nice, France 23–27 Oct. 1995, p. 1295.

32 W. J. Schutte, M. Sluyters-Rehbach and J. H. Sluyters, *J. Phys. Chem.,* 1993, **97**, 6069.

33 M. Fujiki, H. Tabei and T. Kurihara, *J. Phys. Chem*., 1988, **92**, 1281.

34 Similar behaviour has been found for octadodecoxymethyl phthalocyanines: see ref. 10(*b*).

35 K. C. Chang, *J. Heterocycl. Chem*., 1977, **14**, 1285.

36 S.G. Boxer, *Biochim. Biophys. Acta*, 1983, **726**, 265.

37 R. Selensky, D. Holten, M. W. Windsor, J. B. Paine III, D. Dolphin, M. Gouterman and J. C. Thomas, *Chem. Phys*., 1981, **60**, 3.

38 A. Ferencz, D. Neher, M. Schulze, G. Wegner, L. Viaene and F. C. de Schryver, *Chem. Phys. Lett*., 1995, **245**, 23.

39 G. Blasse, G. J. Dirksen, A. Meijerink, J. F. van der Pol, E. Neeleman and W. Drenth, *Chem. Phys. Lett*., 1989, **154**, 420.

40 J. Vacus and J. Simon, *Adv. Mater*., 1995, **7**, 797.

41 Recently, it has been found that Zn-tetrasulfonatoPc forms a face-to-face slipped or tilted dimer in wet acetonitrile which exhibits a red-shifted absorption band and a rather intense fluorescence, while in water a non-emissive face-to-face dimer exists indicated by a strong blue-shifted absorption band relative to the monomeric species: Y. Kaneko, T. Arai, K. Tokumaru, D. Matsunaga and H. Sakuragi, *Chem.Lett*., 1996, 345.

Paper 6/05328I; *Received* 30*th July*, 1996